Enzymes involved in pyrophosphate and calcium metabolism as targets for anti-scuticociliate chemotherapy

Natalia Mallo[a], Jesús Lamas[b], Ana-Paula DeFelipe[a], Rosa-Ana Sueiro[a,b], Francisco Fontenla[b], José-Manuel Leiro[a]

[1]Laboratorio de Parasitología, Instituto de Investigación y Análisis Alimentarios, Universidad de Santiago de Compostela, Santiago de Compostela, Spain.

[2]Departamento de Biología Celular y Ecología and Instituto de Acuicultura, Facultad de Biología, Universidad de Santiago de Compostela, Santiago de Compostela, Spain.

Short Title: Metabolic targets for anti-scuticociliate therapy

Correspondence:

José M. Leiro, Laboratorio de Parasitología, Instituto de Investigación y Análisis Alimentarios, c/ Constantino Candeira s/n, 15782, Santiago de Compostela (A Coruña), Spain; Tel:34981563100; Fax: 34881816070; E-mail: josemanuel.leiro@usc.es

ABSTRACT

Inorganic pyrophosphate (PPi) is a key metabolite in cellular bioenergetics under chronic stress conditions in prokaryotes, protists and plants. Inorganic pyrophosphatases (PPases) are essential enzymes controlling the cellular concentration of PPi and mediating intracellular pH and Ca+2 homeostasis. We report the effects of the antimalarial drugs chloroquine (CQ) and artemisinin (ART) on the in vitro growth of Philasterides dicentrarchi, a scuticociliate parasite of turbot; we also evaluated the action of these drugs on soluble (sPPases) and vacuolar H+-PPases (H+-PPases). CQ and ART inhibited the in vitro growth of ciliates with IC50 values of respectively 74 ± 9 μM and 80 ± 8 μM. CQ inhibits the H+ translocation (with an IC50 of 13.4 ± 0.2 μM), while ART increased translocation of H+ and acidification. However, both drugs caused a decrease in gene expression of H+-PPases. CQ significantly inhibited the enzymatic activity of sPPases, decreasing the consumption of intracellular PPi. ART inhibited intracellular accumulation of Ca+2 induced by ATP, indicating an effect on the Ca2+-ATPase. The results suggest that CQ and ART deregulate enzymes associated with PPi and Ca2+ metabolism, altering the intracellular pH homeostasis vital for parasite survival and providing a target for the development of new drugs against scuticociliatosis.

Keywords: *Philasterides dicentrarchi;* inorganic pyrophosphatases; chloroquine; artemisinin; calcium; intracellular pH.

INTRODUCTION

Inorganic pyrophosphate (PPi) and ATP perform similar functions in terms of energy (Baltscheffsky and Baltscheffsky, 1996). It is believed that the use of PPi as an energy source was acquired earlier in evolution than ATP and that it may be present in cells as PPi or polyphosphate (Kajander *et al*., 2013). PPi, which is mainly generated during biosynthesis of macromolecules, is essential for cellular metabolism, acting as an energy donor and allosteric regulator in many routes and molecular reactions, such as the PPi-dependent phosphorylation of Fru-6-P, catalyzed by phosphofructokinase (PPi-PFK), and PPi-driven proton translocation mediated by H^+ pyrophosphatase (H^+-PPase) (Theodoru and Plaxton, 1993; Pace *et al.,* 2011). Two main different types of PPase have been described: membrane integral H^+ translocating PPase (H^+-PPase) and soluble or cytosolic PPase (sPPase). The latter of these is further classified, on a structural basis, into 3 subtypes: I II and III (Kornberg *et al*, 1962; Pérez-Castiñeira *et al.*, 2002b). PPases differ greatly in both sequence and in structure: sPPases are ubiquitous enzymes that hydrolyze PPi to provide the energy to drive biosynthetic reactions, while membrane PPases use energy produced from the hydrolysis of PPi to move H^+ across the membrane to generate an electrochemical H^+ gradient (Baltscheffsky *et al*., 1999; Pérez-Castiñeira *et al.*, 2002a). PPases can also be classified by their responses to inhibitors such as sodium fluoride (NaF) and bisphosphonates and by the divalent cation required for activity (Mg^{+2} or Mn^{+2}) (Drodowitz *et al.,* 1999; Kajander *et al.,* 2013; Gajadeera *et al.,* 2015). The main similarity between soluble PPases and H^+-PPases is catalytic site structure (Kajander *et al*., 2013). Both types of PPases have been found in a broad range of organisms including protozoan parasites such as *Trypanosoma, Toxoplasma, Plasmodium* and *Leishmania* (Luo *et al*., 1999; McIntosh *et al.,* 2001; Pérez Castiñeira *et al*., 2002b; Gómez-García *et al.,* 2004; Lemercier *et al.,* 2004; Espiau et al., 2006; Sen *et al*, 2009; Pace *et al.,* 2011). An H^+-PPase has recently been

identified in the ciliate parasite *Philasterides dicentrarchi*, the etiological agent of scuticociliatosis in cultured turbot (Mallo *et al.*, 2015). Although type I Mg^{2+}-dependent sPPases are present in all organisms, H^{+}-PPases have not been identified in mammals; they therefore represent a potential therapeutic target for developing new antiprotozoal drugs (Freitas-Mesquita *et al.*, 2014).

Trypanosomatid and apicomplexan parasites possess acidic Ca^{+2} storage organelles, designated acidocalcisomes, with a high PPi content. In association with their membranes, these organelles have several proton-ion exchanger and proton- and Ca^{+2}-pumping ATPases and H^{+}-PPases that are involved in regulation of intracellular pH and osmolarity (Docampo et al., 2013). Disruption of intracellular pH homeostasis has therefore been proposed as a possible route for the development of antiparasitic agents (Jiang et al., 2002). One of the most common antiparasitic compounds is the antimalarial chloroquine (CQ), a weak diprotic base derivative of quinine, which has long been used to prevent malaria (Ponnampalam, 1981). CQ is accumulated in acidic compartments, preferentially in the lysosome and in acidic vacuoles and acidocalcisomes, and the pH level is an essential factor for its accumulation (Bray *et al.*, 2002; Spiller *et al*., 2002). CQ enters these compartments passively by simple diffusion and once inside is protonated (CQ^{+2}) and trapped, thus enabling it to interfere with processes essential to parasite survival, by releasing ROS (López and Segura Latorre, 2008; Li *et al.*, 2014).

Another chemotherapeutic agent against malaria, artemisinin (ART), a secondary metabolite of the plant *Artemisia annua* L., is a known inactivator of channel proteins and causes changes in membrane potential (Golenser *et al*., 2006; Kim *et al.*, 2015) at endoplasmic reticulum and vacuolar membrane levels (Crespo *et al*., 2008; Liu *et al*., 2010). Artemisinin has been identified as a Ca^{2+}-ATPase inhibitor, producing

alterations in cellular Ca^{2+} homeostasis (Ekstein-Ludwig *et al*., 2003; Golenser *et al*., 2006; Shandilya *et al*., 2013); this phenomenon has also been described in other parasites such as *Toxoplasma gondii* (Nagamune *et al*., 2007).

No effective treatment has yet been developed against the scuticociliate *Philasterides dicentrarchi*, which causes serious mortalities in cultured turbot (Iglesias et al., 2001). In this study we evaluated the *in vitro* antiparasitic effects of CQ and ART on this ciliate. We also investigated the role of these agents in the activity of enzymes involved in PPi metabolism and in the regulation of intracellular levels of PPi, osmoregulation, intracellular pH and Ca^{2+} homeostasis.

MATERIAL AND METHODS

Experimental animals

Specimens of the turbot *Scophthalmus maximus*, of approximately 50 g body weight, were obtained from a fish farm in Galicia. The fish were held in 250 L tanks with aerated recirculating seawater maintained at 17-18ºC and under a photoperiod of 12h light/dark. The fish were fed daily with commercial pellets (Skretting, Burgos, Spain) and acclimatized to the aquarium conditions for at least 2 weeks before the start of the experiments.

Parasites and culture

Specimens of the ciliate *P. dicentrarchi* (isolated I1; Budiño *et al.*, 2011) were isolated from naturally infected turbot showing signs of scuticociliatosis. The fish were obtained from a fish farm in Galicia, Spain. The ciliates were aseptically isolated from peritoneal fluid of the turbot, as previously described (Iglesias *et al.*, 2001). The isolated

ciliates were grown at 21° C in complete sterile L-15 medium (Leibovitz, GE HealthCare Europe GmbH, Barcelona, Spain; 10% salinity, pH 7.2) containing 90 mg/L each of adenosine, cytidine and uridine, 150 mg/L of guanosine, 5 g/L of glucose, 400 mg/L of L-α-phosphatidylcholine, 200 mg/L of Tween 80, 10% heat-inactivated foetal bovine serum (FBS) and 10 mL/L of 100X of an antibiotic/antimycotic solution (100 units/ml penicillin G, 0.1 mg/mL streptomycin sulphate and 0.25 mg/mL amphotericin B; Sigma-Aldrich, Madrid, Spain), as previously described (Iglesias *et al*., 2003). In order to maintain the virulence of the ciliates, fish were experimentally infected every 6 months by intraperitoneal injection of 200 µL of sterile physiological saline solution (PSS; 0.15M NaCl) containing 5 x 10^5 ciliates, and ciliates were subsequently obtained from the fish on about the fifth day post infection.

Anti-ciliate activity

The anti-ciliate activity was assayed, as previously described (Mallo *et al*,. 2014). The antimalarial agents CQ and ART (Sigma-Aldrich) were prepared in 100 mM stock solutions, in dimethylsulphoxide (DMSO), and maintained at −20 °C in the dark until use. To investigate the anti-ciliate effects, the antimalarial agents were added to a 96-well sterile culture plate (Corning, Fisher Scientific, Madrid, Spain) containing 15× 10^3 ciliates/mL, to final concentrations between 1 and 100 µM. The plates were then incubated for 3 days at 21 °C. Aliquots (15 µL) of the different treatments/ciliates were removed from each of five replicate wells. After the ciliates were inactivated with 0·25% glutaraldehyde, they were quantified using a haemocytometer (Iglesias *et al*., 2002). To rule out possible effects of DMSO, L-15 medium containing the highest concentration of DMSO used (100 µM) was added to five replicate wells. The *in vitro* inhibitory concentrations (IC_{50}) of the antimalarial agents were calculated using Excel

(Microsoft Office; Microsoft, Madrid, Spain), by plotting the dose response data and applying linear regression (y= mx+b) to fit the data: the values were then calculated from the equation IC_{50} = (0.5-b) x log dose / m, where m is the slope y_1-y_2 / x_1-x_2 and b is the intercept of the line.

Measurement of PPi-driven H^+-transport

The assay was carried out using acridine orange (a cationic fluorescent dye that is accumulated in acidic compartments) as an indicator of transmembrane pH difference in permeabilized ciliates (Rohloff and Docampo, 2006). The assay was performed as previously described (Mallo *et al.,* 2015), with minor modifications. Briefly, 2.5 x 10^5 ciliate cells were collected, permeabilized with digitonin (DIG) to a final concentration of 6.6 µM, and washed twice with PBS. After washing, the pellet was resuspended in assay buffer containing 100 mM KCl, 0.4 M glycerol, 1 mM Tris-EGTA, and 5mM Tris-HCl, 1 mM PMSF and 1 ug/ml leupeptin, pH 8, containing 2.5 µM acridine orange. The reaction was initiated by the addition of Tris-PPi (1 mM) to the medium containing 1.3 mM $MgSO_4$. The kinetics of fluorescence was measured at 485/530 excitation /emission in a fluorimeter (*Fluox800*, BioTek Instruments, Winooski, VT, USA) (Rodrigues *et al.,* 2000; Mallo *et al.,* 2015). A negative control experiment without pyrophosphate was established. Antimalarial agents were added from stock solutions prepared in reaction buffer (Moreno *et al*., 2011). Assays were performed at room temperature.

PPi assay

The PPi assay was carried out with lysates of ciliates cultured for 3 days with different treatments. Briefly, 2 x 10^6 ciliates/mL were washed twice with PBS by centrifugation at 700 x *g* for 5 min and at 4 °C. The pellet was then resuspended in 1 mL of cold distilled water containing 1 mM PMSF and incubated for 15 min on ice. The sample was then sonicated to disrupt the cells (10 cycles of 5 pulses in a W-250 sonifier (Branson Ultrasonic, Danbury, CT, USA) and subsequently centrifuged at 10000 x *g* for 10 min at 4 ºC to eliminate cellular debris. The protein concentration in the lysates was determined by the Bradford method, with BSA as standard. 10 µl of concentrated (10X) sample buffer (30 mM $MgCl_2$, 2 mM EDTA, 2% BSA) was added to the protein solution, which was then filtered through a 10kDa pore filter, Amicon Ultra-0.5 mL (Merck-Millipore, Darmstadt, Germany) to remove endogenous PPi.

PPi was determined with a pyrophosphate reagent kit (Sigma-Aldrich, Madrid, Spain), following the manufacturer's instructions. The test is based on the principle that two moles of NADH are oxidized to NAD, per mole of PPi consumed, by the activity of PPi-dependent fructose 6-phosphate kinase (PFK-PPi). To test the effects of the antimalarial agents, ciliates were incubate for 3 days with 100 µM of CQ, ART and the PPi analogue risdronate (RIS) that was used as a control, and the lysates were obtained as described above. 22 µg of protein per sample of each of three replicates was added to each well of a 96-well UV transparent microplate (Corning, Fisher Scientific, Madrid, Spain); the pyrophosphate reagent was then added, and the reaction was monitored at 340 nm for 10 min in a microplate reader (Biotek EL808, BioTek Instruments, Winooski, VT, US). The final reaction volume was 100 µL and a standard was used at a concentration of 1 mM PPi (O'Brien *et al*., 1976).

Acridine orange staining

Aliquots of $5x10^5$ ciliates were cultured with the different treatments for 30 min and then centrifuged at 700 x *g* for 5 min and washed twice with PBS before being stained (10 min) with a solution of 3 µM acridine orange (Sigma-Aldrich, Madrid, Spain), a fluorophore that selectively accumulates in acidic compartments. The stained ciliates were observed in a fluorescence microscope fitted with an excitation BP 450/490 nm dichroic mirror filter and FT 510 nm LP emission 520 nm filter.

Reverse transcription and real-time polymerase chain reaction (RT-qPCR)

Ciliates were incubated for 24 hours with CQ and ART at the concentrations indicated in the graphs. The total RNA was isolated from 10^7 cells/sample with the NucleoSpin RNA isolation kit (Macherey-Nagel, Düren, Germany) and treated with DNase I (RNase free, Thermo Fisher Scientific, Waltham, MA, USA) before the final concentration and purity were estimated in a NanoDrop ND-1000 spectrophotometer. cDNA synthesis (25 µl/reaction) was performed by a reverse transcription reaction with random primers (1.25 mM) (Roche Custom Biotech, Indianapolis, IN, USA), 250 µM of deoxynucleoside triphosphate (dNTP), 10 mM dithiothreitol (DTT), 20U of RNase inhibitor, 2.3 mM $MgCl_2$ and 200U of reverse transcriptase of Moloney murine leukemia virus (MMLV) (Promega Biotech Ibérica, Madrid, Spain) in buffer containing 30 mM Tris, 20 mM KCl (pH 8.3). The cDNA was generated with 2 µg RNA samples (Mallo *et al.*, 2013).

The qPCR reaction was performed using a reaction mixture already containing the assay buffer and dNTPs, Maxima SYBR Green qPCR Master Mix (Thermo Fisher Scientific, Waltham, MA, USA). Primer pairs were used at a final concentration of 300 nM and 1µl of cDNA was added per well. The final volume of 10 µL/well was completed with RNase free distilled H_2O. The reaction was executed at 95 °C for 5 min,

followed by 40 cycles of 10s at 95 °C and 30s at 60 °C. At the end of this process, melting curve analysis was carried out at 95 °C for 15s, 55 °C for 15 s, and 95 °C for 15 s. The specificity and the size of the PCR products obtained were confirmed by 2% agarose gel electrophoresis. All reactions were carried out in an Eco Real-time PCR system (Illumina, San Diego, CA, USA). The relative quantification of gene expression was determined by the $2^{-\Delta\Delta Cq}$ method (Livak and Schmittgen, 2001) following minimum information guidelines for publishing real-time quantitative PCR experiments (MIQE) (Bustin *et al.*, 2009). The following primer sequences of H^+-PPase gene were used: Forward/reverse, 5'-GCCTACGAAATGGTCGAAGA-3'/5'-GCATCGGTGTATTGTCCAGA-3'. Gene expression was normalized with the reference gene β-tubulin of *P. dicentrarchi* (forward/reverse primer sequence, 5′-ACCGGGGAATCTTAAACAGG-3′/5′-GCCACCTTATCCGTCCACTA-3′), and the normalized data were expressed in relative arbitrary units. The values show the mean ± the standard error (SE) of three trials.

Primer pairs were designed and optimized with the Primer 3 Plus program (http://www.bioinformatics.nl/cgibin/primer3plus/primer3plus.cgi) with a Tm of 60 °C. (Mallo *et al.*, 2013)

Intracellular Ca^{2+} determination

The ciliates were washed twice, by centrifugation at 700 x*g* for 5 min, and resuspended in assay medium (1X HBSS without Ca^{2+}, 20 mM HEPES and 2.5 mM probenecid) to a final concentration of 1.25 x 10^6 ciliates/mL. The ciliates were then incubated with different treatments for 1 hour in a 96-well plate at 21° C and at the concentrations indicated in the graphs. After incubation, the ciliates were then washed twice with assay medium and the Ca^{2+} probe, Fluo-4 NW (No Wash, Fluo-4 NW

calcium assay kit, Life Technologies) was added, following manufacturer's instructions, and fluorescence (Ex: 494nm, Em: 516nm) was measured in a fluorimeter (*FLx800*, BioTek Instruments, Winooski, VT, USA). Negative controls without the Ca^{2+} probe Fluo-4 NW were established (Paredes *et al*., 2008).

Statistical analysis

Results shown in the figures are expressed as means ± standard error. Significant differences ($P = 0.05$) were determined by analysis of variance (ANOVA) followed by Tukey - Kramer multiple comparison tests.

RESULTS

In vitro effect on ciliate growth

Both CQ (Fig. 1A) and ART (Fig. 1B) treatments significantly inhibited *in vitro* growth of *P. dicentrarchi* in L-15 medium supplemented with 10% FBS for 3 days, indicating antiparasitic effects. The inhibitory effect of CQ and ART on growth of the ciliates was significantly different from that of controls after day 2 of culture (logarithmic growth phase of the culture): IC_{50} = 55.14 ± 4.59 μM for CQ (Fig. 1A), and IC_{50} = 61.10 ± 5.12 μM for ART (Fig. 1B). On day 3 of culture, i.e. when trophozoites were about to enter the stationary phase of growth, the inhibitory activity of both drugs decreased and the IC_{50} values increased (74.36 ± 9.42 μM for CQ and 80.41 ± 7.9 for ART); the latter value is significantly different from that obtained for the first day of culture (Figs. 1A, B).

Effect on PPi-driven H^+ translocating activity and intracellular pH

The effects of CQ (1, 5 and 25 μM) and of ART (25, 50 and 100 μM) on H^+ translocation induced by PPi and intracellular pH are shown in Fig. 2A. CQ significantly inhibited H^+ translocation at all concentrations tested, with a IC_{50} of 13.4 ± 0.2 μM (Fig. 2A), and ART produced a significant increase in the translocation of H^+ at concentrations above 25 μM (Fig. 2B).

Acridine orange staining revealed that the antimalarials had contrasting effects, which also differed from the effects observed in controls (ciliates not treated with antimalarials) (Fig. 2C). Thus, 25 μM CQ caused alkalinization of the ciliates (all endocytic vacuoles stained green); decreasing the concentration of CQ caused an increase in intracellular acidification and yellow-stained endocytic vacuoles were observed (Fig. 3C; upper images in the panel). The ciliates treated with ART at 25 and 100 μM showed a clear increase in intracellular acidification relative to controls, with numerous endocytic vacuoles stained bright red/orange. Acidification levels in endocytic vacuoles decreased at lower doses of ART (Fig. 3C, lower panel images).

Effect of H^+-PPase gene expression

Ciliates cultured for 24 hours with different concentrations (25-100 μM) of both antimalarial agents showed a decrease in H^+-PPase gene expression, relative to the β-tubulin gene, as determined by RT-qPCR (Fig. 3). Both CQ (Fig. 3A) and ART (Fig. 3B) were effective at doses of 50 μM, with IC_{50} values of 44.34 μM (CQ) and 57.3 μM (ART).

Effect of antimalarial agents on PPi levels and role of the PPi analogue risedronate (RIS) on H^+-PPase enzyme activity, gene expression and *in vitro* growth of the parasite

PPi levels were tested after 3 days of treatment of the ciliates with CQ and ART and with the PPi analogue RIS as an inhibitor control. CQ and RIS significantly decreased PPi levels, while ART did not produce any variation in PPi levels, indicating that PPi had not been consumed and that this compound does not affect the sPPases of the parasite (Fig. 4A). The bisphosphonate RIS, at a concentration of 100 μM, also significantly inhibited H^+-PPase activity (Fig. 4B), gene expression (Fig. 4C) and *in vitro* growth of the parasite from the first day of culture (initiation of the logarithmic phase of growth) until day 3 (entry into the stationary phase of growth); however, the IC50 values decreases between day 1 (51.25 ± 5.07 μM) and day 3 (37.29 ± 5.87 μM) (Fig. 4D).

Effect on levels of intracellular Ca^{2+} induced by ATP

Regulation of intracellular Ca^{2+} was studied by the addition of ATP, which is thought to act on the Ca^{2+}-dependent enzyme Ca^{2+}-ATPase. ART is a known inhibitor of this enzyme in apicomplexan and kinetoplastid parasites (Nagamune *et al.*, 2007; Mishina et al., 2007; Tanabe et al., 2011). To study the effect of ART on the scuticociliate *P. dicentrarchi*, Ca^{2+} and ATP (the enzyme substrate) were added to the cultures. In the assay, ciliates were incubated with the different treatments for 1 hour before the Ca^{2+} probe (Fluo-4 NW) was added, and fluorescence was measured 1 hour later. The intracellular Ca^{2+} levels increased significantly in ciliates incubated with ATP and $CaCl_2$ (Fig. 5). Treatment with ART decreased the levels of intracellular Ca^{2+} (Fig. 5B). However, treatment with CQ did not have any effect on the increased intracellular Ca^{2+} levels induced by $CaCl_2$ and ATP (Fig. 5A), indicating that this antimalarial agent does not act at the Ca^{2+}-ATPase level.

DISCUSSION

The antimalarial agents CQ and ART inhibited *P. dicentrarchi* growth, indicating the potential usefulness of these drugs in treating scuticociliatosis. The antiparasitic potential of ART has previously been described in ciliates such as *Tetrahymena thermophila,* in which growth was modulated (Shen *et al.,* 2010). The effect of antimalarial drugs on *P. dicentrarchi* may occur at the levels of pH homeostasis, as CQ has been described as an alkalinizing agent in several parasites (Gazarini *et al.,* 2007). Addition of cationic drugs such as CQ causes rapid alkalization of acidocalcisomes and acidic vacuoles, which will lead to deregulation of the activity of enzymes present in these compartments (Vercesi and Docampo, 1996; Dzekunov et al, 2000; Vercesi et al., 2000). The enzymes located in these compartments could therefore be targets for the antimalarial drug. Although some studies suggest that CQ may activate the membrane transporter Na^+/H^+, this hypothesis is very controversial (Wunsch et al., 1998; Bray et al., 1999; Vercesi et al., 2000).

There is evidence that ART exerts its antimalarial activity at least partly by generating oxidative stress (Krungkrai and Yuthavong, 1987; Klonis et al., 2011). Addition of H_2O_2 to parasites leads to acidification of the parasite cytosol and alkalinization of the digestive vacuole by direct inhibition of the H^+-pumping V-type H^+-ATPase, but does not affect the activity of the H^+-pumping PPase (van Schalwyk et al., 2013). However, ART increased the PPi-driven translocation activity in *P. dicentrarchi,* which may also deregulate pH but with further vacuolar acidification, as observed in the acridine orange assay, in which ciliates treated with ART contained more acidic vacuoles than the control, in contrast with CQ, which has formerly been described to discharge acridine orange from acidic stores in other parasites such as *Plasmodium chabaudi* (Gazarini *et al.,* 2007).

Malarian parasites have been described to have an H^+-PPase and an H^+-ATPase that affect pH control in both the cytosol and the internal digestive vacuole (Marchesini *et al.,* 2000). When parasites are exposed to CQ, H^+ extrusion interferes in pH regulation so that the expression of enzymes involved in pH maintenance may be modulated (Saliba *et al.,* 2003). Thus, *P. falciparum* treated with sublethal concentrations of CQ for 3 days showed upregulation of the expression of two genes involved in vacuolar acidification: H^+-ATPase and an K^+-independent H^+-PPase *PfVp2* (McIntosh et al., 2001; Mwai *et al.,* 2012). Nevertheless, H^+-ATPase has not yet been identified in *P. dicentrarchi,* and the H^+-PPase, after treatment for 24h with CQ, was downregulated. Altogether the results obtained with *P. dicentrarchi* seem to indicate this enzyme as a potential CQ target, as CQ inhibits PPi-driven H^+-translocation and downregulates H^+-PPase expression. In a recent study, H^+-PPase enzyme has been suggested to be involved in CQ resistance (Jovel *et al*., 2014). Our results indicate, for the first time, the involvement of this enzyme in CQ mechanism of action in the ciliate *P. dicentrarchi.*

The inhibitory effect of ART on the gene expression of *P. dicentrarchi* H^+-PPase could be explained as a defence mechanism of the ciliate to prevent upregulation of intravacuolar pH generated by the enzyme. However, as discussed below, the deregulation is probably indirect due to the effect of ART on other enzymes present in endocytic vacuoles and not on H^+-PPase (van Schalwyk et al., 2013).

sPPases have been suggested as potential chemotherapeutic targets as they are involved in growth and infection in parasites such as *T. gondii, Leishmania* and *T. brucei* (Lemercier *et al.,* 2004; Espiau *et al.,* 2006; Pace *et al*., 2011). However, as sPPase sequences have not been characterized in *P. dicentrarchi,* further sequencing studies are required. H^+-PPase inhibitors, such as PPi analogues (bisphosphonates) have

been shown to exert antiprotozoal effects and they are thus being investigated as possible targets for future development of chemotherapeutic treatments (Docampo and Moreno, 2008; Sen *et al*., 2009). Bisphosphanates may act as inhibitors of enzymes that use PPi as a substrate, and several studies have demonstrated the action of PPi in inhibiting H^+-PPase in protozoa such as *T. gondii* (Zhen *et al*., 1994; Docampo and Moreno, 2001; Szabo *et al.,* 2001; Drosdowicz *et al.*, 2003; Kotsikorou *et al.,* 2005). This has also recently been described in the H^+-PPase of *P. dicentrarchi* (Mallo *et al.*, 2015). Our data also shows the ability of bisphosphonates to inhibit sPPases, triggering a decrease in the levels of PPi consumed in cells incubated in the presence of bisphosphonate risedronate (RIS), a phenomenon also described in *T. gondii* (Rodrigues et al., 2000). Addition of CQ, which inhibits PPi-driven H^+ transport, has also been found to cause a decrease in PPi consumption in the ciliate.

Maintenance of pH homeostasis is important for parasite survival (Glaser et al., 1988; Gazarine et al., 2007). Our data show the ability of both antimalarial agents to modify the dynamics of PPi metabolism in *P. dicentrarchi,* indicating a broad effect on ion homeostasis in parasites, including that of Ca^{2+}, which regulates a wide range of functions. The antimalarial agents CQ and ART may exert their antiparasitic effects at this level, modifying pH by regulating enzymes involved in the maintenance and interfering in Ca^{2+} homeostasis. ART has been described as an inhibitor of Ca^{2+}-ATPase (Uhlemann *et al*., 2005; Nagamune *et al*., 2007), which controls Ca^{2+} levels, and among many other activities, exo and endocytosis (Plattner, 2014; Docampo and Huang, 2015). In *Paramecium,* Ca^{2+}-ATPase has been described in the endoplasmic reticulum and in the alveolar sacs, and in *E. histolytica* it has been found in membranes and internal vesicles (Hauser *et al.,* 1998; Kissmehl *et al.,* 1998; Plattner and Klauker, 2001; Nagamune *et al.,* 2007; Plattner *et al.,* 2012). At the membrane level, the Ca^{2+}-ATPase

of *Paramecium* is activated to remove Ca^{2+} when the concentration is relatively high (Stelly *et al*., 1995). In animals and plants, high concentrations of extracellular ATP increase cytoplasmic Ca^{2+} concentrations. Extracellular ATP can also induce ROS production and increase mRNA levels in genes regulated by Ca^{2+} stress (Jeter and Roux, 2006). Although the Ca^{2+}-ATPase enzyme has not been described in *P. dicentrarchi*, the addition of ART has been found to prevent an increase in intracellular Ca^{2+} levels when ATP and Ca^{2+} are added to the medium, suggesting that the enzyme may be present in the ciliate. Previous results obtained in *P. dicentrarchi* indicate that Ca^{2+} is mainly stored in alveolar sacs and acidic vacuoles (results not shown), suggesting that Ca^{2+} uptake in acidic vesicles may be mediated by a Ca^{2+}-ATPase. This enzyme has been reported to interfere with virulence in other parasites (Luo *et al.*, 2004; Galizzi *et al.*, 2013). As demonstrated in other parasites, Ca^{2+} may be also modulated by a Ca^{2+}/H^{+} counter-transporter located in the membrane of the acidocalcisomes (Rohloff *et al.*, 2011), but at the moment this has not been described in *P. dicentrarchi*.

Increased H^{+}-translocation brought about by ART may be related to its role as a Ca^{2+}-ATPase inhibitor, which cannot release H^{+} outside vacuoles after being inactivated. This may be why H^{+}-PPase is downregulated, as it would be not necessary to maintain vacuolar pH levels under such conditions; H^{+}-PPase may therefore be secondarily regulated. On the other hand, CQ also downregulates H^{+}-PPase expression, but alkalinizes the internal vesicles, showing that it acts at a different level than ART in H^{+}-PPase regulation. CQ may act directly on H^{+}-PPase but not on Ca^{2+}-ATPase, inducing alkalinization of the vesicles. Ca^{2+}-ATPase may be associated with Na^{+}/H^{+} and Ca^{2+}/H^{+} transporters, as previously described in acidocalcisomes (Docampo *et al.*, 2005); however, as already mentioned, these enzymes have not been described in *P. dicentrarchi*.

In conclusion, this study shows that the antimalarial drugs CQ and ART exert an antiparasitic effect *in vitro* on the scuticociliate parasite *P. dicentrarchi*, which is at least partly related to their ability to deregulate enzyme activity associated with PPi and Ca^{+2} metabolism. This alters both Ca^{2+} and intracellular pH homeostasis in the ciliate and negatively affects growth. The present findings also suggest the potential role of these enzymes as chemotherapeutic targets for developing new drugs against scuticociliatosis.

ACKNOWLEDGEMENT

This study was financially supported by grant AGL2014-57125-R from the Ministerio de Economía y Competitividad (Spain), by the European Commission, under the Horizon 2020 programme (Grant Agreement 634429, PARAFISHCONTROL), and by grant GPC2014/069 from the Xunta de Galicia (Spain).

LITERATURE CITED

Baltscheffsky, H. & Baltscheffsky, M. 1996. Evolutionary, kinetic and thermodynamic aspects on the bioenergetics of inorganic pyrophosphate (PPi) and adenosine triphosphate (ATP). *Chemical Evolution: Physics of the Origin and Evolution of Life*. pp 145-150

Baltscheffsky, M., Schultz, A. & Baltscheffsky, H. 1999. H^+-PPases a tightly membrane- bound family. *FEBS Lett.*, 457:527-533.

Bray, P.G., Ward, S.A. & Ginsburg, H. 1999. Na^+/H^+ antiporter, chloroquine uptake and drug resistance: inconsistencies in a newly proposed model. *Parasitol. Today*, 15:360-363.

Bray, P.G., Saliba, K.J., Davies, J.D., Spiller, D.G., White, M.R., Kirk, K. & Ward, S.A.

2002. Distribution of acridine orange fluorescence in *Plasmodium falciparum*-infected erythrocytes and its implications for the evaluation of digestive vacuole pH. Mol. Biochem. Parasitol., 119:301-304.

Budiño B, Lamas J, Pata MP, Arranz JA, Sanmartín ML, Leiro J. (2011). Intraspecific variability in several isolates of *Philasterides dicentrarchi* (syn. *Miamiensis avidus*), a scuticociliate parasite of farmed turbot. *Veterinary Parasitology*, **175**:260-72.

Bustin, S.A., Benes, V., Garson, J.A., Hellemans, J., Huggett, J., Kubista, M., Mueller, R., Nolan, T., Pfaffl, M.W., Shipley, G.L., Vandesompele, J., Wittwer, C.T. 2009. The MIQE guidelines: minimum information for publication of quantitative real-time PCR experiments. Clin. Chem., 55:611-622.

Crespo, M.P., Avery, T.D., Hanssen, E., Fox, E., Robinson, T.V., Valente, P., Taylor, D.K. & Tilley, L. 2008. Artemisinin and a series of novel endoperoxide antimalarials exert early effects on digestive vacuole morphology. Antimicrob. Agents Ch., 52:98-109.

Docampo, R., de Souza, W., Miranda, K., Rohloff, R., & Moreno, S.N.J. 2005. Acidocalcisomes –conserved from bacteria to man. Nat. Rev. Microbiol.**,** 3:251-261.

Docampo, R., Jimenez, V., Lander, N., Li, Z.H., Niyogi, S. 2013. New insights into roles of acidocalcisomes and contractile vacuole complex in osmoregulation in protists. Int. Rev. Cell Mol. Biol., 305:69-113.

Docampo, R. & Moreno, S.N. 2001. The acidocalcisome. Mol. Biochem. Parasitol., 114:151-159.

Docampo, R. & Moreno, S.N. 2008. The acidocalcisome as a target for chemotherapeutic agents in protozoan parasites. Curr. Pharm. Design,

14:882-888.

Docampo, R. & Huang, G. 2015. Calcium signaling in trypanosomatid parasites. Cell Calcium, 57: 194-202.

Drozdowicz, Y.M., Lu, Y.P., Patel, V., Fitz-Gibbon, S., Miller, J.H. & Rea, P.A. 1999. A thermostable vacuolar-type membrane pyrophosphatase from the archaeon *Pyrobaculum aerophilum*: implications for the origins of pyrophosphate-energized pumps. FEBS Lett., 460:505-512.

Drozdowicz, Y.M., Shaw, M., Nishi, M., Striepen, B., Liwinski, H.A., Roos, D.S. & Rea, P.A. 2003. Isolation and characterization of TgVP1, a type I vacuolar H^+-translocating pyrophosphatase from *Toxoplasma gondii*. The dynamics of its subcellular localization and the cellular effects of a diphosphonate inhibitor. J. Biol. Chem., 278:1075-1085.

Dzekunov, S.M., Ursos, L.M. & Roepe, P.D. 2000. Digestive vacuolar pH of intact intraerythrocytic *P. falciparum* either sensitive or resistant to chloroquine. Mol. Biochem. Parasitol. 110:107-124.

Eckstein-Ludwig, U., Webb, R.J., Van Goethem, I.D., East, J.M., Lee, A.G., Kimura, M., O'Neill, P.M., Bray, P.G., Ward, S.A. & Krishna, S. (2003). Artemisinins target the SERCA of *Plasmodium falciparum*. Nature, 424:957-961.

Espiau, B., Lemercier, G., Ambit, A., Bringaud, F., Merlin, G., Baltz, T. & Bakalara, N. 2006. A soluble pyrophosphatase, a key enzyme for polyphosphate metabolism in *Leishmania*. J. Biol. Chem., 281:1516-1523.

Freitas-Mesquita, A.L., Fonseca-de-Souza, A.L. & Meyer-Fernandes, J.R. 2014. *Leishmania amazonensis*: Characterization of an ecto-pyrophosphatase activity. Exp. Parasitol., 137:8–13.

Gajadeera, C.S., Zhang, X., Wei, Y. & Tsodikov, O.V. 2015. Structure of inorganic

525 pyrophosphatase from *Staphylococcus aureus* reveals conformational flexibility
526 of the active site. J. Struct. Biol., 189:81-86.
527 Galizzi, M., Bustamante, J.M., Fang, J., Miranda, K., Soares Medeiros, L.C., Tarleton,
528 R.L. & Docampo, R. 2013. Evidence for the role of vacuolar soluble
529 pyrophosphatase and inorganic polyphosphate in *Trypanosoma cruzi*
530 persistence. Mol. Microbiol., 90:699-715.
531 Gazarini, M.L., Sigolo, C.A., Markus, R.P., Thomas, A.P. & García, C.R. 2007.
532 Antimalarial drugs disrupt ion homeostasis in malarial parasites. Mem. I.
533 Oswaldo Cruz, 102:329-334.
534 Glaser, T.A., Baatz, J.E., Kreishman, G.P. & Mukkada, A.J. 1988. pH
535 homeostasis in *Leishmania donovani* amastigotes and promastigotes. Proc. Natl.
536 Acad. Sci. U. S. A., 85:7602-7606.
537 Golenser, J., Waknine, J.H., Krugliak, M., Hunt, N.H. & Grau, G.E. 2006. Current
538 perspectives on the mechanism of action of artemisinins. Int. J. Parasitol., 36:
539 1427–1444.
540 Gómez-García, M.R., Ruiz-Pérez, L.M., González-Pacanowska, D. & Serrano, A. 2004.
541 A novel calcium-dependent soluble inorganic pyrophosphatase from the
542 trypanosomatid *Leishmania major*. FEBS Lett., 560:158-166.
543 Hauser, K., Pavlovic, N., Kissmehl, R. & Plattner, H. 1998. Molecular characterization
544 of a sarco(endo)plasmic reticulum Ca2+-ATPase gene from *Paramecium*
545 *tetraurelia* and localization of its gene product to sub-plasmalemmal calcium
546 stores. Biochem. J. 334:31-38.
547 Iglesias, R., Paramá, A., Álvarez, M.F., Leiro, J., Fernández, J. & Sanmartín, M.L.
548 2001. *Philasterides dicentrarchi* (Ciliophora, Scuticocilatida) as the causative
549 agent of scuticociliatosis in farmed turbot *Scophthalmus maximus* in Galicia

(NW Spain). Dis. Aquat. Organ., 46:47–55.

Iglesias, R., Paramá, A., Álvarez, M.F., Leiro, J. & Sanmartín, M.L. 2002. Antiprotozoals effective *in vitro* against the scuticociliate fish pathogen *Philasterides dicentrarchi*. Dis. Aquat. Organ. 49:191-197.

Iglesias, R., Paramá, A., Álvarez, M.F., Leiro, J., Aja, C. & Sanmartín, M.L. 2003. *In vitro* growth requirements for the fish pathogen *Philasterides dicentrarchi* (Ciliophora, Scuticociliatida). Vet. Parasitol., 111:19-30.

Jeter, C.R. & Roux, S.J. 2006. Plant responses to extracellular nucleotides: Cellular processes and biological effects. Purinergic Signal., 2:443-449.

Jiang, S., Meadows, J., Anderson, S.A. & Mukkada, A.J. 2002. Antileishmanial activity of the antiulcer agent omeprazole. Antimicrob. Agents Ch., 46:2569-2574.

Jovel, I.T., Ferreira, P.E., Veiga, M.I., Malmberg, M., Mårtensson, A., Kaneko, A., Zakeri, S., Murillo, C., Nosten, F., Björkman, A. & Ursing, J. 2014. Single nucleotide polymorphisms in *Plasmodium falciparum* V type H(+) pyrophosphatase gene (pfvp2) and their associations with pfcrt and pfmdr1 polymorphisms. Infect. Genet. Evol., 24:111-115.

Kajander, T., Kellosalo, J. & Goldman, A. 2013. Review Inorganic pyrophosphatases: One substrate, three mechanisms. FEBS Lett., 587:1863-1869.

Kim, W.S., Choi, W.J., Lee, S., Kim, W.J., Lee, D.C., Sohn, U.D., Shin, H.S. & Kim, W. (2015). Anti-inflammatory, antioxidant and antimicrobial effects of artemisinin extracts from *Artemisia annua* L. Korean J. Physiol. Pharm., 19:21-27.

Kissmehl, R., Huber, S., Kottwitz, B., Hauser, K. & Plattner, H. 1998. Subplasmalemmal Ca-stores in *Paramecium tetraurelia*. Identification and

575 characterisation of a sarco(endo)plasmic reticulum-like Ca^{2+}-ATPase by
576 phosphoenzyme intermediate formation and its inhibition by caffeine. Cell
577 Calcium, 24:193-203.
578 Klonis, N., Crespo-Ortiz, M.P., Bottova, I., Abu-Bakar, N., Kenny S, Rosenthal, P.J. &
579 Tilley L. 2011. Artemisinin activity against *Plasmodium falciparum* requires
580 hemoglobin uptake and digestion. Proc. Natl. Acad. Sci. U.S.A., 108:11405–
581 11410.
582 Kotsikorou, E., Song, Y., Chan, J.M., Faelens, S., Tovian, Z., Broderick, E., Bakalara,
583 N., Docampo, R. & Oldfield, E. 2005. Bisphosphonate inhibition of the
584 exopolyphosphatase activity of the *Trypanosoma brucei* soluble vacuolar
585 pyrophosphatase. J. Med. Chem., 48:6128-6139.
586 Kornberg, A. 1962. On the metabolic significance of phosphorolytic and
587 pyrophosphorolytic reactions. In Horizonts in Biochemistry. Kasha, M. &
588 Pullman, B, eds., (251-264). Academic Press, New York.
589 Krungkrai, S.R. & Yuthavong, Y. 1987. The antimalarial action on *Plasmodium*
590 *falciparum* of qinghaosu and artesunate in combination with agents which
591 modulate oxidant stress. Trans. R. Soc. Trop. Med. Hyg., 81:710–714.
592 Leiro, J., Piazzón, M.C., Budiño, B., Sanmartín, M.L. & Lamas, J. 2008. Complement-
593 mediated killing of *Philasterides dicentrarchi* (Ciliophora) by turbot serum:
594 relative importance of alternative and classical pathways. Par. Immunol.,
595 30:535-543.
596 Lemercier, G., Espiau, B., Ruiz, F.A., Vieira, M., Luo, S., Baltz, T., Docampo, R. &
597 Bakalara, N. 2004. A pyrophosphatase regulating polyphosphate metabolism in
598 acidocalcisomes is essential for *Trypanosoma brucei* virulence in mice. *J. Biol.*
599 *Chem.*, 279:3420-3425.

600 Li, F.J. & He, C.Y. 2014. Acidocalcisome is required for autophagy in *Trypanosoma*
601 *brucei*. Autophagy, 10:1978-1988.
602 Liu, Q., Zhang, Q., Burton, R.A., Shirley, N.J. & Atwell, B.J. 2010. Expression of
603 vacuolar H+- pyrophosphatase (OVP3) is under control of an anoxia-inducible
604 promoter in rice. Plant Mol. Biol., 72:47-60.
605 Livak, K.J. & Schmittgen, T.D. 2001. Analysis of relative gene expression data using
606 real-time quantitative PCR and the $2^{-\Delta\Delta CT}$ method. Methods 25:402-408.
607 López, M.L. & Segura Latorre, C. 2008. The new permeability pathways and cytosolic
608 pH: targets for antimalarial agents on *Plasmodium falciparum*. Acta Biol.
609 Colomb., 13: 3-22.
610 Luo, S., Marchesini, N., Moreno, S.N. & Docampo, R. 1999. A plant-like vacuolar
611 H(+)- pyrophosphatase in *Plasmodium falciparum*. FEBS Lett., 460:217-220.
612 Luo, S., Rohloff, P., Cox, J., Uyemura, S.A. & Docampo, R. 2004. *Trypanosoma brucei*
613 plasma membrane-type Ca(2+)-ATPase 1 (TbPMC1) and 2 (TbPMC2) genes
614 encode functional Ca(2+)-ATPases localized to the acidocalcisomes and plasma
615 membrane, and essential for Ca(2+) homeostasis and growth. J. Biol. Chem.,
616 279:14427-14433.
617 Mallo, N., Lamas, J. & Leiro, J. 2013. Hydrogenosome metabolism is the key target for
618 antiparasitic activity of resveratrol against *Trichomonas vaginalis*. Antimicrob.
619 Agents Ch., 57:2476-2484.
620 Mallo, N., Lamas, J. & Leiro, J.M. 2014.Alternative oxidase inhibitors as antiparasitic
621 agents against scuticociliatosis. Parasitology, 141:1311-1321.
622 Mallo, N., Lamas, J., Piazzon, C. & Leiro, J.M. 2015. Presence of a plant-like proton-
623 translocating pyrophosphatase in a scuticociliate parasite and its role as a
624 possible drug target. Parasitology, 142:449-462.

625 Marchesini, N., Luo, S., Rodrigues, C.O., Moreno, S.N. & Docampo, R. 2000.
626 Acidocalcisomes and a vacuolar H+-pyrophosphatase in malaria parasites.
627 Biochem. J., 347:243-253.
628 McIntosh, M.T., Drozdowicz, Y.M., Laroiya, K., Rea, P.A. & Vaidya, A.B. 2001. Two
629 classes of plant-like vacuolar-type H(+)-pyrophosphatases in malaria parasites.
630 Mol. Biochem. Parasitol., 114:183-195.
631 Mishina, Y.V., Krishna, S., Haynes, R.K. & Meade, JC. 2007. Artemisinins inhibit
632 *Trypanosoma cruzi* and *Trypanosoma brucei rhodesiense in vitro* growth.
633 Antimicrob. Agents Ch., 51:1852-1854.
634 Moreno, S.N.J., Ayong, L. & Pace, D.A. 2011. Calcium storage and function in
635 apicomplexan parasites. Essays Biochem. Vol., 51:97-110.
636 Mwai, L., Diriye, A., Masseno, V., Muriithi, S., Feltwell, T., Musyoki, J., Lemieux, J.,
637 Feller, A, Mair, G.R., Marsh, K., Newbold, C., Nzila, A. & Carret, C.K. 2012.
638 Genome wide adaptations of *Plasmodium falciparum* in response to
639 lumefantrine selective drug pressure. PLoS One, 7:e31623.
640 Nagamune, K., Beatty, W.L. & Sibley, L.D. 2007. Artemisinin induces calcium-
641 dependent protein secretion in the protozoan parasite *Toxoplasma gondii*.
642 Eukaryot. Cell, 6:2147-2156.
643 O'Brien, W.E. 1976. A continuous spectrophotometric assay for arininosuccinate
644 synthetase based on pyrophosphate formation. Anal. Biochem., 76:423-403.
645 Pace, D.A., Fang, J., Cintron, R., Docampo, R. & Moreno, S.N. 2011. Overexpression
646 of a cytosolic pyrophosphatase (TgPPase) reveals a regulatory role of PP(i) in
647 glycolysis for *Toxoplasma gondii*. Biochem. J., 440:229-240.
648 Paramá, A., Iglesiass R., Álvarezs M.F., Leiro, J., Aja, C. & Sanmartín, M.L. 2003.
649 *Philasterides dicentrarchi* (Ciliophora, Scuticociliatida): experimental infection

and possible routes of entry in farmed turbot (*Scophthalmus maximus*). *Aquaculture,* 217: 73–80.

Paredes, R.M., Etzler, J.C., Watts, L.T., Zheng, W., & Lechleiter, J.D. (2008). Chemical calcium indicators. *Methods*, **46**:143–151.

Pérez-Castiñeira, J.R., López-Marqués, R.L., Villalba, J.M., Losada, M. & Serrano, A. (2002a). Functional complementation of yeast cytosolic pyrophosphatase by bacterial and plant H^+-translocating pyrophosphatases. Proc. Nat. Acad. Sci. U.S.A., 99:15914-15919.

Pérez-Castiñeira, J.R., Alvar, J., Ruiz-Pérez, L.M. & Serrano, A. 2002b. Evidence for a wide occurrence of proton-translocating pyrophosphatase genes in parasitic and free-living protozoa. Biochem. Biophys. Res. Commun., 294: 567-573.

Plattner, H. & Klauke, N. 2001. Calcium in Ciliated Protozoa: Sources, Regulation, and Calcium-Regulated Cell Functions. *Int. Rev.* Cytol., 201:115-208.

Plattner, H., Sehring, I.M., Mohamed, I.K., Miranda, K., De Souza, W., Billington, R., Genazzani, A. & Ladenburger, E.M. 2012. Calcium signaling in closely related protozoan groups (Alveolata): non-parasitic ciliates (*Paramecium, Tetrahymena*) vs. parasitic Apicomplexa (*Plasmodium, Toxoplasma*). Cell Calcium, 51:351-382.

Plattner, H. (2014). Calcium signalling in the ciliated protozoan model, *Paramecium*: Strict signal localisation by epigenetically controlled positioning of different Ca^{2+}-channels. *Cell Calcium*, 57:203-213.

Ponnampalam, J.T. 1981. Chemotherapy of malaria. Ann Acad Med Singapore., 10:99-106.

Rodrigues, C.O., Scott, D.A., de Souza, BN, Benchimol, W., Urbina, J., Oldfield, M.A & Moreno S.N. (2000). Vacuolar proton pyrophosphatase activity (PPi) in

675 *Toxoplasma gondii* as possible chemotherapeutic target. Biochem. J. 349: 737-
676 745.
677 Rohloff, P. & Docampo, R. 2006. Ammonium production during hypo-osmotic stress
678 leads to alkalinization of acidocalcisomes and cytosolic acidification in
679 *Trypanosoma cruzi*. Mol. Biochem. Parasitol. 150:249–255.
680 Rohloff, P., Miranda, K., Rodrigues, J.C., Fang, J., Galizzi, M., Plattner, H., Hentschel,
681 J. & Moreno, S.N. 2011. Calcium uptake and proton transport by
682 acidocalcisomes of *Toxoplasma gondii*. PLoS One, 6:e18390.
683 Saliba, K.J., Allen, R.J., Zissis, S., Bray, P.G., Ward, S.A. & Kirk, K. 2003.
684 Acidification of the malaria parasite's digestive vacuole by a H+-ATPase and a
685 H+-pyrophosphatase. J. Biol. Chem., 278:5605-5612.
686 Sen, S.S., Bhuyan, N.R. & Bera, T. 2009. Characterization of plasma membrane
687 bound inorganic pyrophosphatase from *Leishmania donovani* promastigotes and
688 amastigotes. Afr. Health Sci., 9:212-217.
689 Shen, X.S., Su, Q., Qiu, Z.P., Xu, J.Y., Xie, Y.X., Liu, H.F. & Liu, Y. 2010. Effects of
690 artemisinin derivative on the growth metabolism of *Tetrahymena thermophila*
691 BF5 based on expression of thermokinetics. Biol. Trace Elem. Res., 136:117-25.
692 Shandilya, A., Chacko, S., Jayaram, B. & Ghosh, I. 2013. A plausible mechanism for
693 the antimalarial activity of artemisinin: A computational approach. Sci. Rep., 3:
694 2513.
695 Stelly, N., Halpern, S., Nicolas, G., Fragu, P. & Adoutte, A. 1995. Direct visualization
696 of a vast cortical calcium compartment in *Paramecium* by secondary ion mass
697 spectrometry (SIMS) microscopy: possible involvement in exocytosis. *J. Cell*
698 *Sci.*, 108:1895-1909.
699 Spiller, D.G., Bray, P.G., Hughes, R.H., Ward, S.A. & White, M.R. 2002. The pH of the

Plasmodium falciparum digestive vacuole: holy grail or dead-end trail? Trends Parasitol., 18.:441-444.

Szabo, C.M. & Oldfield, E. 2001. An investigation of bisphosphonate inhibition of a vacuolar proton-pumping pyrophosphatase. Biochem. Biophys. Res. Commun., 287:468-473.

Tanabe, K., Zakeri, S., Palacpac, N.M., Afsharpad, M., Randrianarivelojosia, M., Kaneko, A., Marma, A.S., Horii, T. & Mita, T. 2011. Spontaneous mutations in the *Plasmodium falciparum* sarcoplasmic/ endoplasmic reticulum Ca^{2+}-ATPase (PfATP6) gene among geographically widespread parasite populations unexpose d to artemisinin-based combination therapies. Antimicrob Agents Ch. 55:94-100.

Theodorou, M.E. & Plaxton, W.C. 1993. Metabolic adaptations of plant respiration to nutritional phosphate deprivation. Plant Physiol., 101: 339-344.

Uhlemann, A.C., Cameron, A., Eckstein-Ludwig, U., Fischbarg, J., Iserovich, P., Zuniga, F.A., East, M., Lee, A., Brady, L., Haynes, R.K. & Krishna, S. 2005. A single amino acid residue can determine the sensitivity of SERCAs to artemisinins. Nat. Struct. Mol. Biol., 12:628-629.

Van Schalkwyk, D.A., Saliba, K.J., Biagini, G.A., Bray, P.G. & Kirk, K. 2013. Loss of pH control in *Plasmodium falciparum* parasites subjected to oxidative stress. PLoS One, 8:e58933.

Vercesi, A.E. & Docampo, R. 1996. Sodium proton exchange stimulates Ca2+ release from acidocalcisomes of *Trypanosoma brucei*. Biochem. J., 315:265-70.

Vercesi, A.E., Rodrigues, C.O., Catisti, R. & Docampo, R. 2000. Presence of a Na(+)/H(+) exchanger in acidocalcisomes of *Leishmania donovani* and their

alkalization by anti-leishmanial drugs. FEBS Lett., 473:203-206.

Wünsch, S., Sánchez, C.P., Gekle, M., Grosse-Wortmann, L., Wiesner, J. & Lanzer, M. 1998. Differential stimulation of the Na^+/H^+ exchanger determines chloroquine uptake in *Plasmodium falciparum*. J. Cell. Biol., 140:335-345.

Zhen, R.G., Kim, E.J. & Rea, P. 1997. The molecular and biochemical basis of pyrophosphatase energized proton translocation at the vacuolar membrane. Adv. Bot. Res., 25: 297-337.

Figures

Figure 1: *In vitro* growth of *P. dicentrarchi* in L-15 supplemented with 10% FBS and with the antimalarial agents A) chloroquine (CQ) and B) artemisinin (ART). To determine the effect of drugs on the growth of ciliates (lines) and to calculate the IC_{50} values (bars), ciliates were incubated for three days with five concentrations of the drugs (1-100 μM). Each point on the graph (symbols and bars) represents the mean ± standard error. **P*<0.05, **P<0.01 relative to untreated controls (*n*= 5); ^{a}P <0.05 relative to IC_{50} on first day.

Figure 2: Effects of (A) chloroquine (CQ) at concentrations of 1, 5 and 25 μM and (B) artemisinin (ART) at concentrations of 25, 50 and 100 μM on PPi-driven H^+ translocation. Δ represents the change in fluorescence, calculated in arbitrary units/sec (mean ± standard error; n = 5) from the time that the antimalarial agent was added until the end of the assay. The mean values ± standard error of the IC_{50} obtained in this assay are shown in the top right box in Figure A. **P*<0.05, ***P*<0.01 relative to the control in each case. C) Photomicrographs of trophozoites of *P. dicentrarchi* stained with the pH sensitive fluorescent dye acridine orange and incubated with 1 and 25 μM CQ (upper panel) and 25 and 100 μM ART (lower panel). Acidic intracellular compartments are stained in colours ranging from yellow (less acidic) to orange / red (more acid), while alkaline compartments are stained green.

Figure 3: Effect of the antimalarial agents (A) chloroquine (CQ) and (B) artemisinin (ART) on relative gene expression of H^+-PPase enzyme. Ciliate cultures were incubated for 24 h with different doses of CQ and ART (25, 50 and 100 μM). Data are expressed in arbitrary units standardized to the β-tubulin reference gene as the mean ± standard error (*n* = 3). ** *P* < 0.01 relative to each of the controls.

772

773 **Figure 4:** A) Concentration of PPi consumed, determined using PPi reagent (SIGMA)
774 and spectrophotometric measurement for 10 min of lysates obtained from ciliates
775 cultivated during 3 days with 100 μM of chloroquine (CQ), artemisinin (ART) or
776 risedronate (RIS). B) Effect of the PPi analogue RIS, at a concentration of 100 μM, on
777 PPi-driven H^+ translocation. Δ represents the change in fluorescence, calculated in
778 arbitrary units/sec. C) Effect of RIS (100 μM) on relative gene expression of H^+-PPase.
779 Data are expressed in arbitrary units standardized to the β-tubulin reference gene. D)
780 Effect of RIS, at concentrations between 1-100 μM, on trophozoite growth (line graph)
781 during three days. The IC_{50} values obtained are indicated on the bars in the graph. Data
782 are mean values ± standard error (*n* = 5), and asterisks indicate the statistical
783 significance: **P* <0.05 and ***P*< 0.01 relative to the untreated control.
784

785 **Figure 5:** Intracellular Ca^{2+} levels obtained with the Fluo-4 NW probe. Effects of A)
786 Artemisinin (ART) and B) chloroquine (CQ) on ciliates cultivated for 1 hour with 100
787 μM of the antimalarial agents and 1 mM ATP. Bars represent the mean values ±
788 standard error (n= 5) of fluorescence in arbitrary units. ** *P* <0.01
789

Figure 1

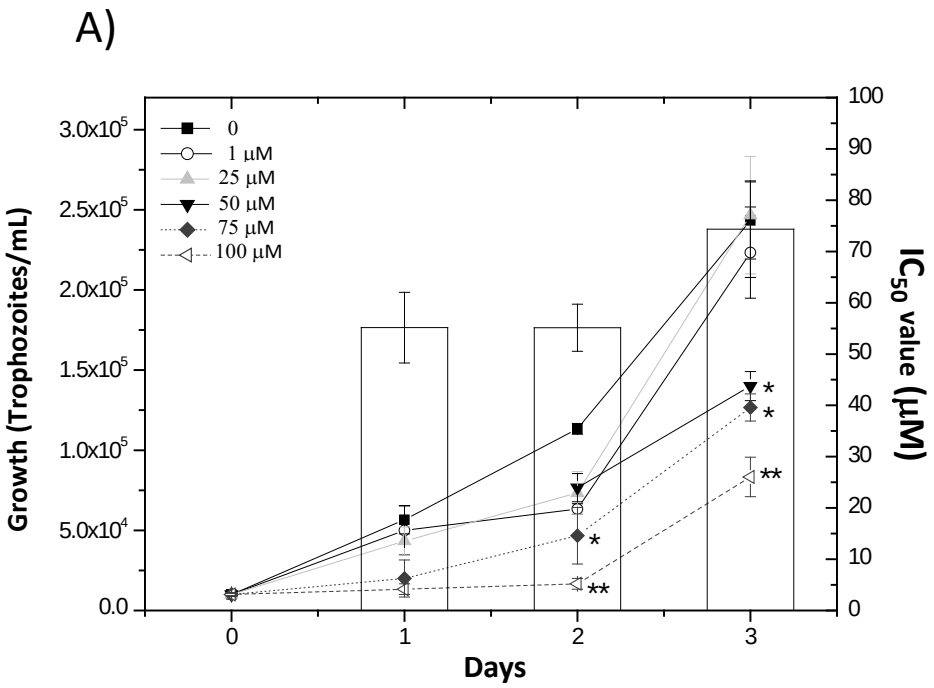
A)
0
1 µM
25 µM
50 µM
75 µM
100 µM
Growth (Trophozoites/mL)
IC50 value (µM)
Days
3.0x10^5
2.5x10^5
2.0x10^5
1.5x10^5
1.0x10^5
5.0x10^4
0.0
100
90
80
70
60
50
40
30
20
10
0
0
1
2
3
*
*
*
**
**

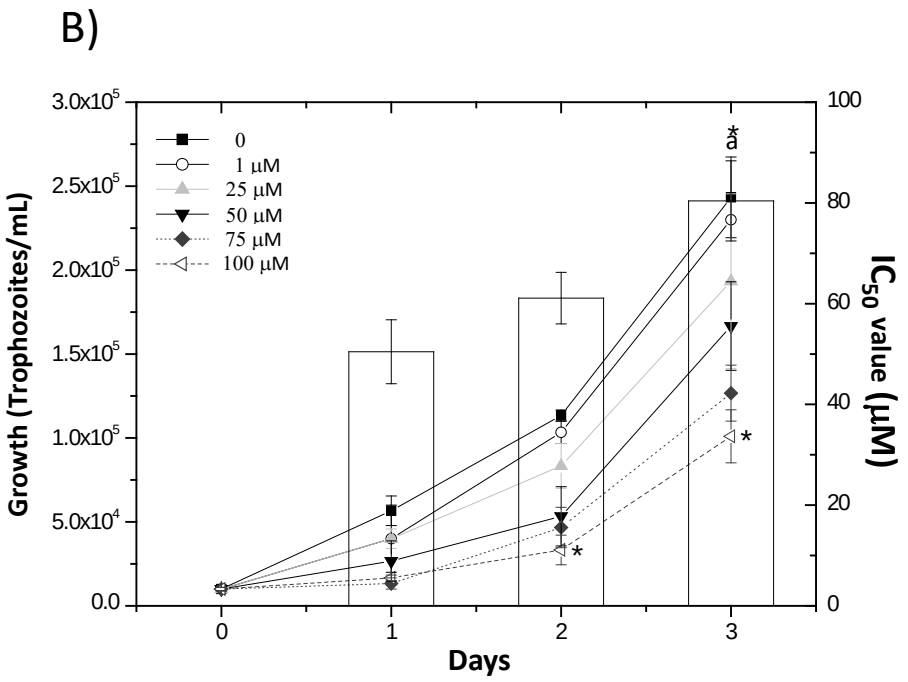
B)
0
1 µM
25 µM
50 µM
75 µM
100 µM
Growth (Trophozoites/mL)
IC50 value (µM)
Days
3.0x10^5
2.5x10^5
2.0x10^5
1.5x10^5
1.0x10^5
5.0x10^4
0.0
100
80
60
40
20
0
0
1
2
3
a
*
*
*

A)

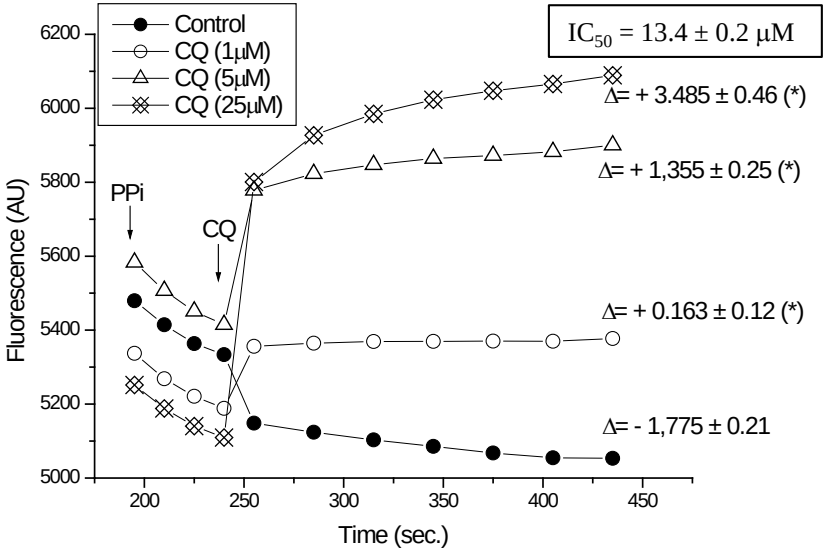
Control
CQ (1μM)
CQ (5μM)
CQ (25μM)
IC50 = 13.4 ± 0.2 μM
Δ= + 3.485 ± 0.46 (*)
Δ= + 1,355 ± 0.25 (*)
Δ= + 0.163 ± 0.12 (*)
Δ= - 1,775 ± 0.21
PPi
CQ
Fluorescence (AU)
Time (sec.)

B)

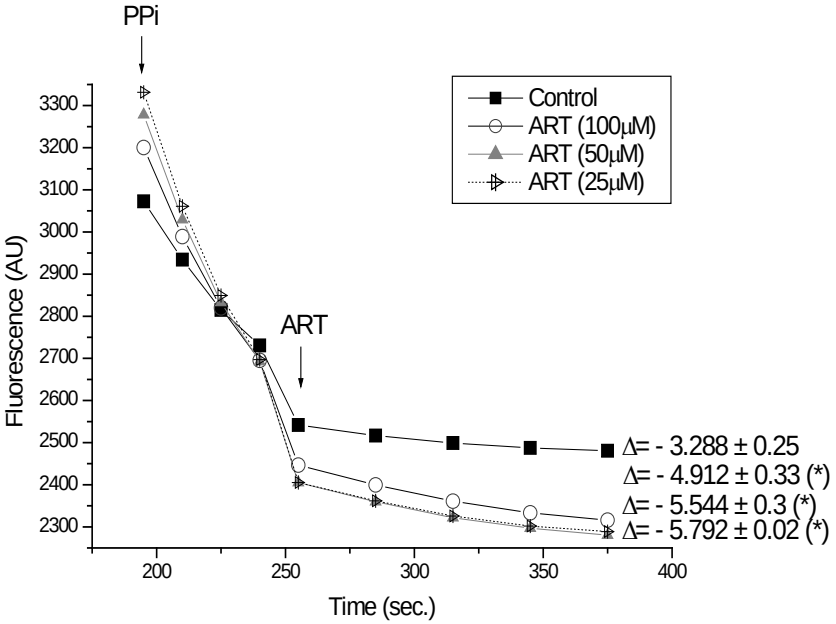
PPi
Control
ART (100μM)
ART (50μM)
ART (25μM)
ART
Δ= - 3.288 ± 0.25
Δ= - 4.912 ± 0.33 (*)
Δ= - 5.544 ± 0.3 (*)
Δ= - 5.792 ± 0.02 (*)
Fluorescence (AU)
Time (sec.)

C)

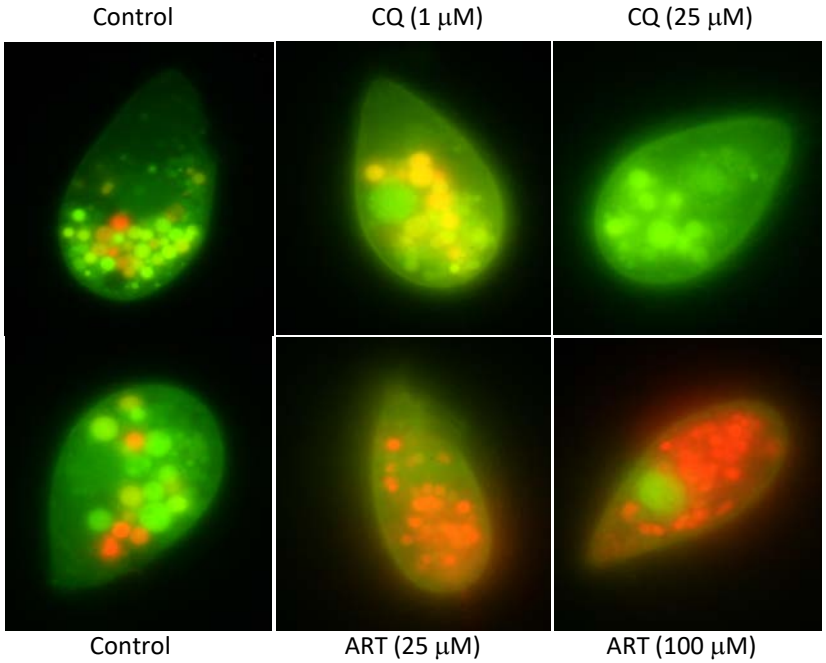
Control
CQ (1 μM)
CQ (25 μM)
Control
ART (25 μM)
ART (100 μM)

Figure 2

Figure 3

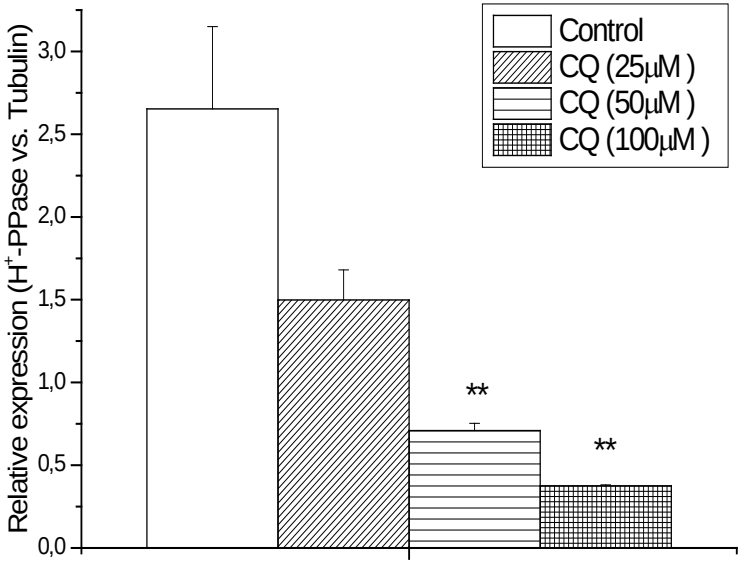
Relative expression (H+-PPase vs. Tubulin)
3,0
2,5
2,0
1,5
1,0
0,5
0,0
Control
CQ (25μM)
CQ (50μM)
CQ (100μM)
**
**

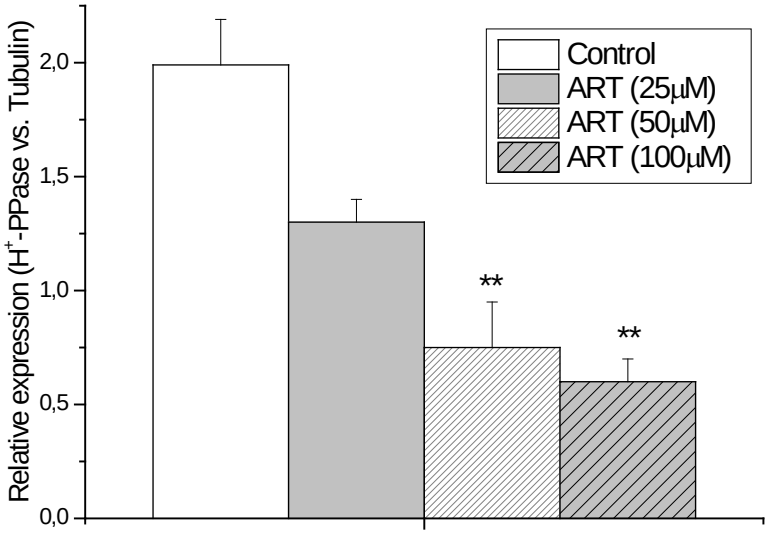
Relative expression (H+-PPase vs. Tubulin)
2,0
1,5
1,0
0,5
0,0
Control
ART (25μM)
ART (50μM)
ART (100μM)
**
**

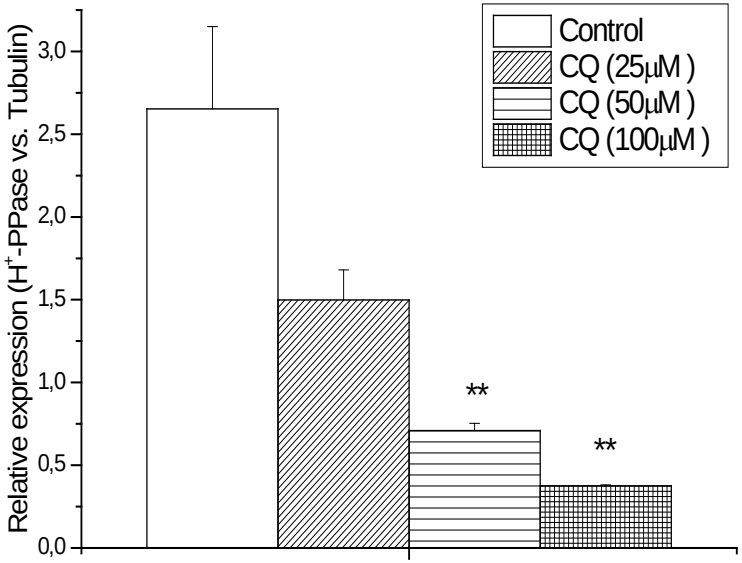
Control
CQ (25μM)
CQ (50μM)
CQ (100μM)
Relative expression (H+-PPase vs. Tubulin)
3,0
2,5
2,0
1,5
1,0
0,5
0,0
**
**

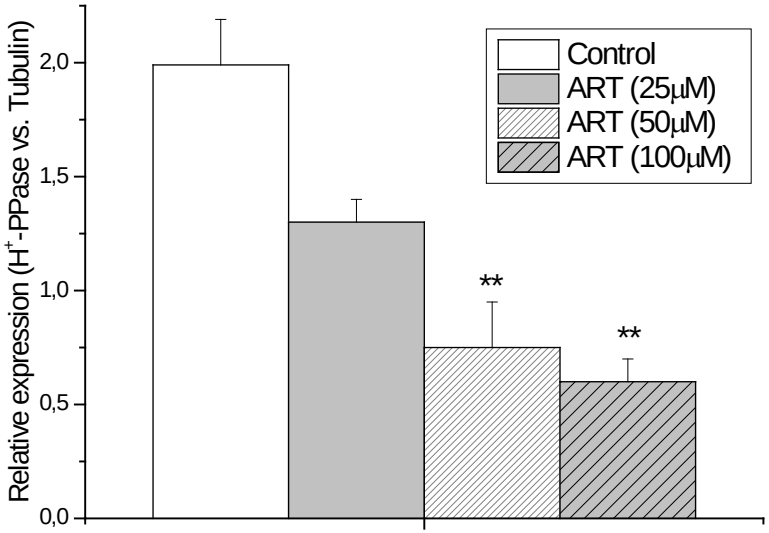
Control
ART (25μM)
ART (50μM)
ART (100μM)
Relative expression (H+-PPase vs. Tubulin)
2,0
1,5
1,0
0,5
0,0
**
**

Figure 4

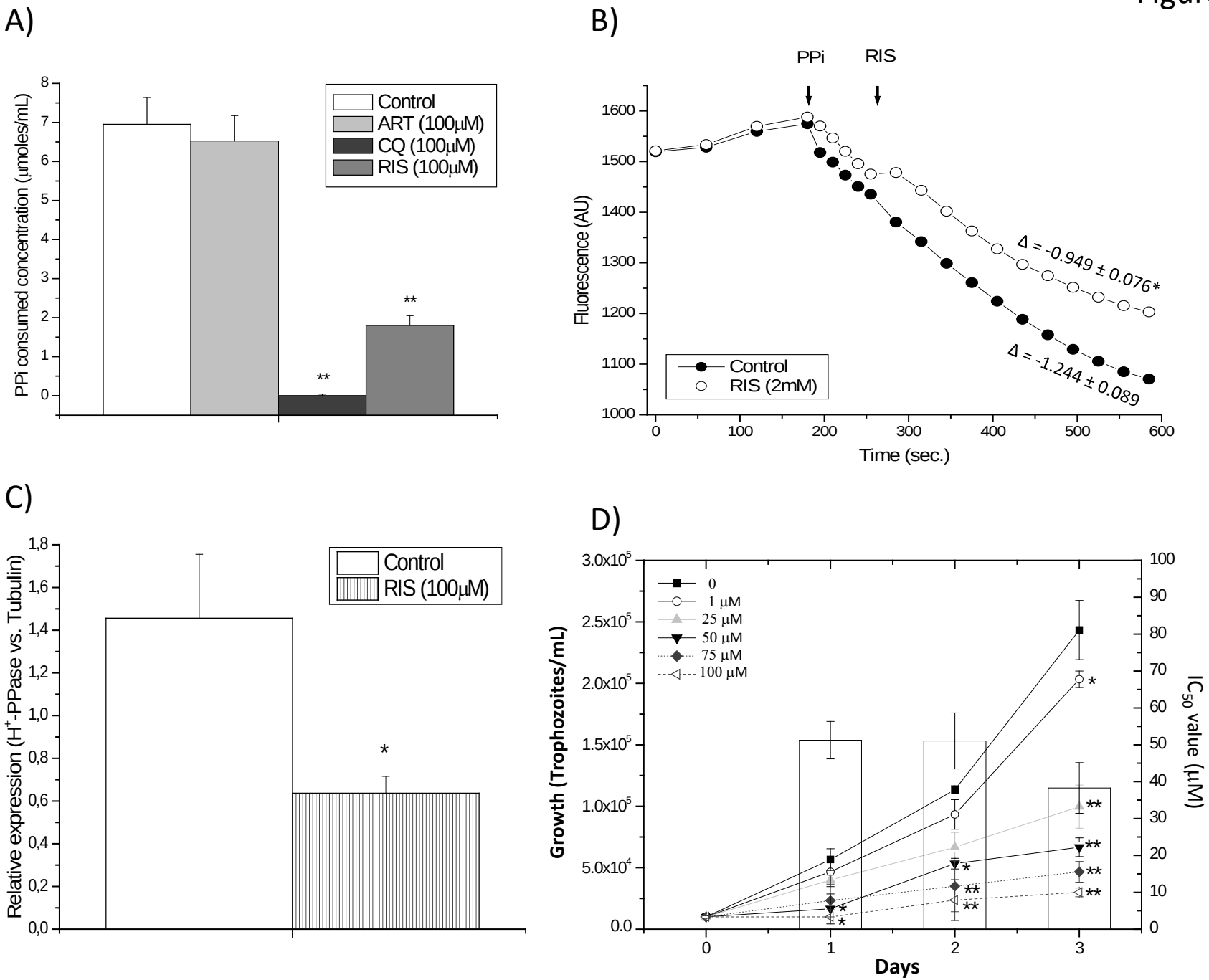
A)
PPi consumed concentration (µmoles/mL)
Control
ART (100µM)
CQ (100µM)
RIS (100µM)
**
**
B)
PPi
RIS
Fluorescence (AU)
Time (sec.)
Control
RIS (2mM)
Δ = -0.949 ± 0.076*
Δ = -1.244 ± 0.089
C)
Relative expression (H+-PPase vs. Tubulin)
Control
RIS (100µM)
*
D)
Growth (Trophozoites/mL)
IC50 value (µM)
Days
0
1 µM
25 µM
50 µM
75 µM
100 µM

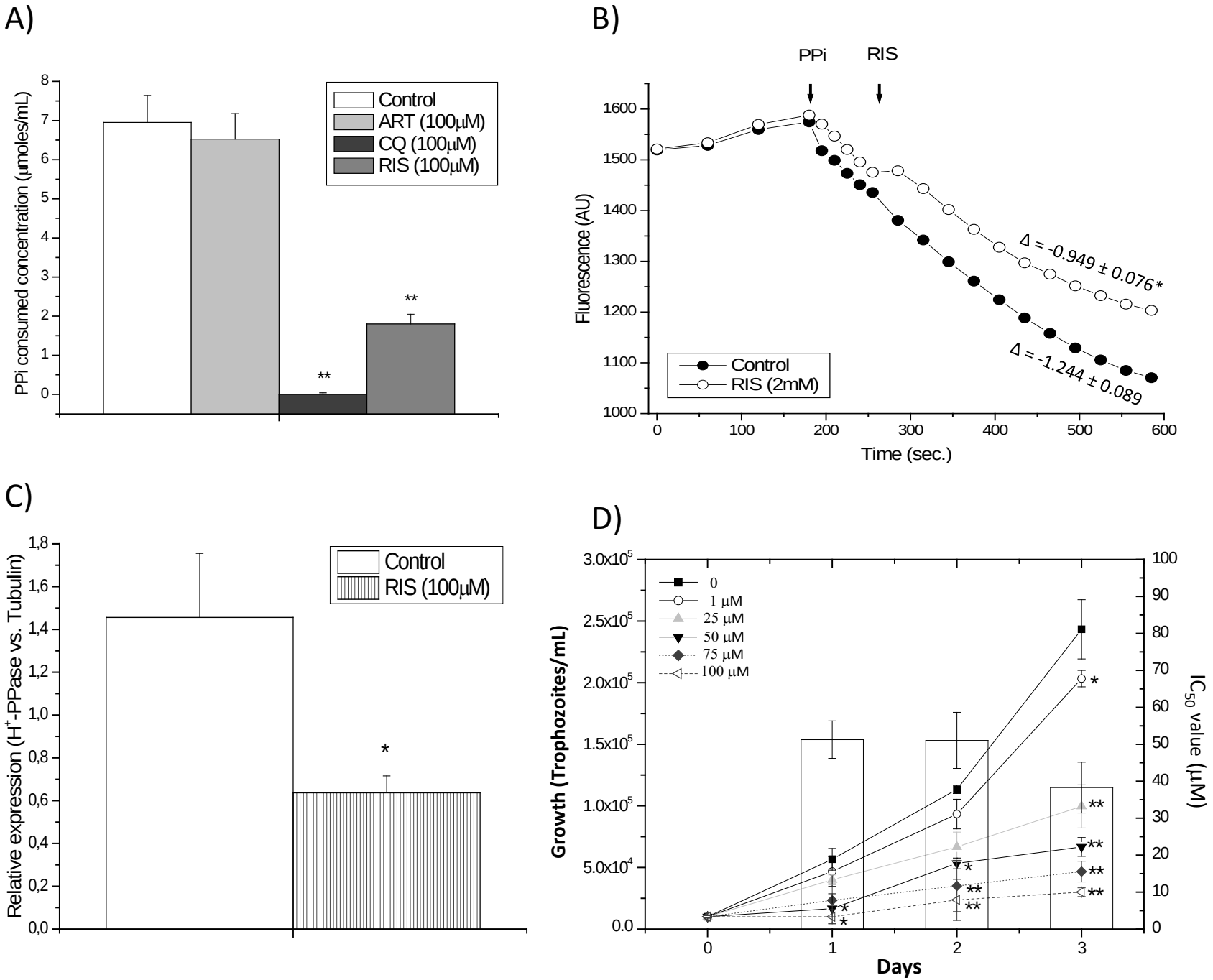
A)
PPi consumed concentration (µmoles/mL)
Control
ART (100µM)
CQ (100µM)
RIS (100µM)
**
**
B)
PPi
RIS
Fluorescence (AU)
Time (sec.)
Control
RIS (2mM)
Δ = -0.949 ± 0.076*
Δ = -1.244 ± 0.089
C)
Relative expression (H+-PPase vs. Tubulin)
Control
RIS (100µM)
*
D)
Growth (Trophozoites/mL)
IC50 value (µM)
Days
0
1 µM
25 µM
50 µM
75 µM
100 µM

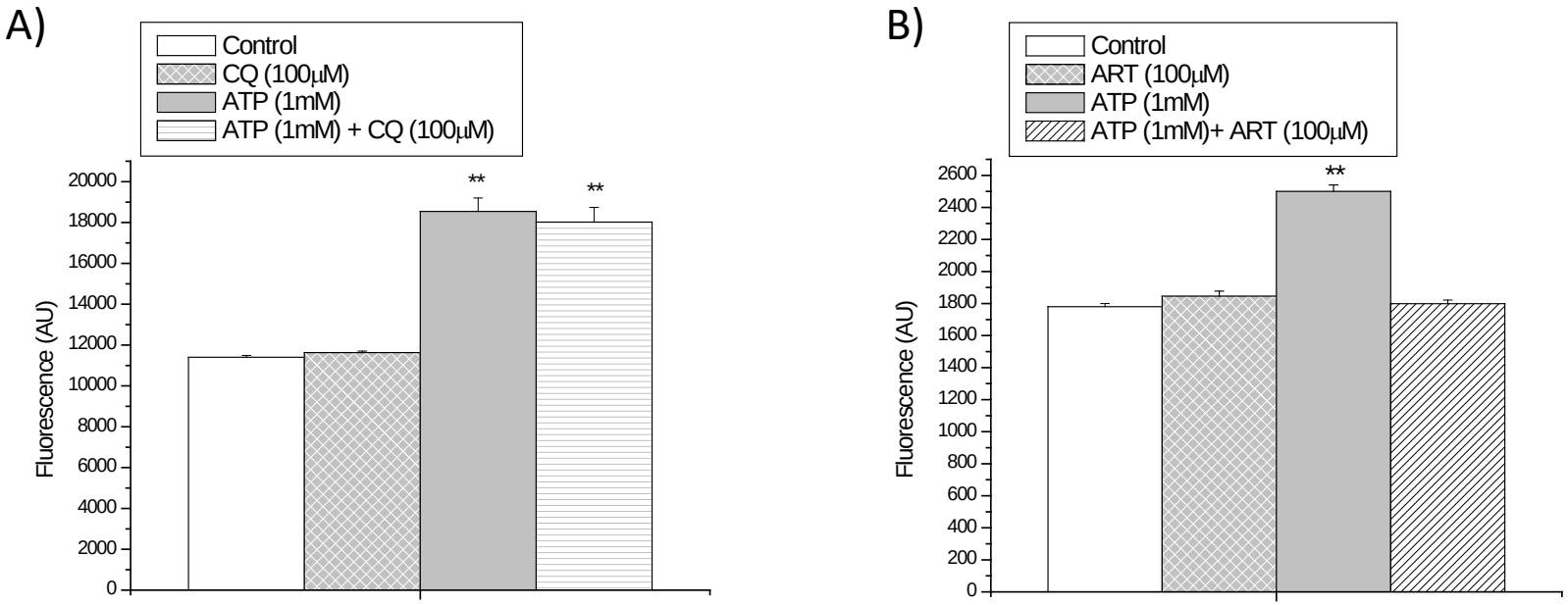
A)
Control
CQ (100μM)
ATP (1mM)
ATP (1mM) + CQ (100μM)
Fluorescence (AU)
0
2000
4000
6000
8000
10000
12000
14000
16000
18000
20000
**
**
B)
Control
ART (100μM)
ATP (1mM)
ATP (1mM)+ ART (100μM)
Fluorescence (AU)
0
200
400
600
800
1000
1200
1400
1600
1800
2000
2200
2400
2600
**